The Case of Formic Acid on Anatase TiO2(101): Where is the Acid Proton?

To be cited as: **Angew. Chem. Int. Ed. 10.1002/anie.201906709**

The case of HCOOH on (101) anatase TiO_2: where is the acid proton?

Gloria Tabacchi,[a] Marco Fabbiani,[b] Lorenzo Mino,[b] Gianmario Martra,[b] and Ettore Fois*[a]

Abstract: Carboxylic acids adsorption on anatase TiO_2 is a relevant process in many technological applications. Yet, in spite of several decades of investigations, the acid proton localization – either on the molecule or on the surface – is still an open issue. By modeling the adsorption of formic acid on top of (101) anatase surfaces, we highlight the formation of a short-strong hydrogen bond. In the 0 K limit, the acid proton behavior is ruled by quantum delocalization effects in a single potential well, while at room conditions the proton undergoes a rapid classical shuttling in a shallow two-wells free energy profile. This picture, supported by agreement with available experiments, shows that the anatase surface acts like a protecting group for the carboxylic acid functionality. Such a new conceptual insight might help rationalize chemical processes involving carboxylic acids on oxide surfaces.

Atomistic insight of adsorbed –COOH groups on TiO_2 is of key relevance in photocatalysis and environmental remediation processes.[1] Moreover, the interaction of carboxylic groups with TiO_2 governs the anchoring of solar cell sensitizers.[2] Also, TiO_2 catalyzes solvent-free direct amidation of R-COOH with amines,[3] and amino acid oligomerization in prebiotic conditions.[4] Atmospheric carboxylic acids show an impressive adsorption selectivity on rutile TiO_2 (110) with respect to alcohols, present in much higher concentrations.[5] This behavior, proposed to affect self-cleaning and photocatalytic properties of TiO_2, was rationalized by the atomistic details of the formate dissociative adsorption in a bidentate mode.[5,6] Conversely, for anatase, which is the preferred TiO_2 form in many applications, the adsorption of small carboxylic acids still shows puzzling aspects.[7] This holds true also for the most stable (101) surface - the principal termination of anatase nanoparticles[7,8] - even for stoichiometric samples with low density of defects. One of the main issues stems indeed from IRRAS and STM experiments dealing with the adsorption of HCOOH[9] and H_3C-COOH,[10] respectively, on non-defective terminations of anatase (101) single crystals. In both cases, the features related to the HCOO/H_3C-COO moieties pointed toward dissociative adsorption. However, neither IRRAS nor STM studies gave clear indications of the acid proton fate: no νOH signal was detected by IRRAS, and no surface OH were found by STM. So, a simple, but fundamental question arises: where is the missing proton?

Here we report that the acid proton is shared between the -COO^- group and a surface oxygen, and forms a short-strong-hydrogen-bond (SSHB). The proton behavior is ruled by quantum delocalization at low temperature and by thermally activated shuttling at room temperature. This picture, obtained from modeling yet in line with experiments, suggests that the catalytic oxide surface acts as a protecting group of the Brønsted acid functionality.

To trace the proton fate, we focus on regular non-defective anatase (101), which is an archetype in TiO_2 surface science and displays the unsolved problem of the proton location. Also, accurate experimental data are available,[9,10] against which our predictions may be validated. Hence, we explore different anchoring geometries for HCOOH with first principles molecular dynamics (FPMD),[11,12] as thermal effects play a key role at molecule-material interfaces.[8,13]

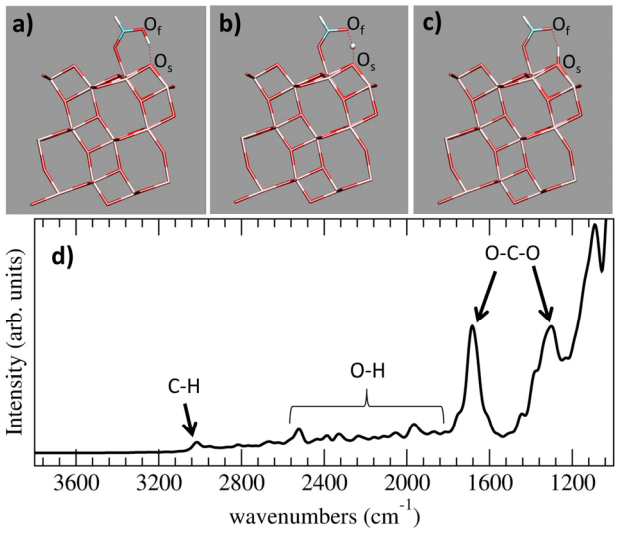

Figure 1. a-c: Snapshots from a 300 K simulation of monodentate HCOOH on TiO_2(101); **a)** undissociated HCOOH strongly H-bonded to a surface oxygen O_s; **b)** formate-TiO_2 proton shuttling; **c)** O_s is protonated and strongly H-bonded to formate. **d)** IR spectrum calculated from this trajectory. Wavenumbers were scaled using a scaling factor of 1.0678 (see SI).

The starting point was a structure proposed on the basis of IRRAS spectra,[9] depicting the dissociation of HCOOH in a $HCOO^-$ monodentate to a surface Ti (Ti_s) and a proton transferred to an oxygen atom of the surface (O_s), not interacting with formate (see SI for details on models setup). This system resulted thermally unstable: after few ps of FPMD at 300 K, the $HCOO^-$(Ti) and $H^+(O_s)$ adducts relaxed to undissociated HCOOH monodentate to a Ti_s. Moreover, the $H^+(O_s)$ stretching mode shows a well defined frequency (3621 cm^{-1}), whereas no νOH signal was detected by IRRAS.[9] Attention was then turned to the 300 K trajectories where HCOOH keeps monodentate adsorption with one oxygen bonded to a 5-coordinated Ti (Figure 1a-c). Interestingly, the other carboxyl oxygen O_f - initially protonated, forming an OH moiety H-bonded to a surface oxygen O_s- is, on average, only transiently protonated at 300 K, as the acid proton shuttles between O_f and O_s (see movie M1). The spectroscopic signature of this regime is a very broad, low-intensity band in the 2500-1800 cm^{-1} range (Figure 1d; see Figure S4 for other simulated IR

[a] G. Tabacchi, E. Fois
Department of Science and High Technology
University of Insubria and INSTM
via Valleggio 9, I-22100 Como, Italy
E-mail: *ettore.fois@uninsubria.it*
[b] M. Fabbiani, L. Mino, G.Martra
Department of Chemistry and Nanostructured Interfaces and Surfaces NIS interdepartmental centre
University of Torino
via P. Giuria 7, I-10125 Torino, Italy

Supporting information for this article is given via a link at the end of the document

patterns), likely difficult to be observed experimentally. The calculated O-C-O vibrational features are in good agreement with IRRAS data (see Table 1). Low νOH frequencies are peculiar of strong H-bonds X··H··Y in molecular systems with short X-Y distances,[14] and of proton sharing in condensed phases.[15] As a matter of fact, the average O_f-O_s distance in our simulation is 2.484 Å, typical of SSHB.

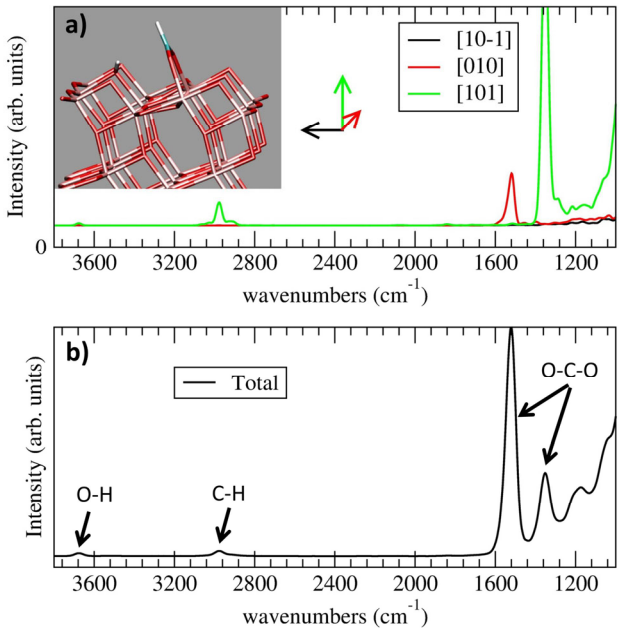

Figure 2. a) Inset: Snapshot from a 300 K simulation of bridging formate on TiO_2(101). Vibrational spectra: FT of the autocorrelation function for the three dipole moment components. **b)** IR spectrum calculated by FT of the total dipole moment autocorrelation function. Wavenumbers were scaled using a scaling factor of 1.0678 (see SI).

For validation, we considered a stable dissociative adsorption of HCOOH, namely a formate ($HCOO^-$) moiety on a protonated (101) facet in a bidentate bridging mode. Calculated IR signals are shown in Figure 2 (see Figure S4 for other simulated IR patterns). Among the IR components (Figure 2a), we notice a strong [010] signal, which should correspond to a strong negative IRRAS band.[9] Such band and the ν(OH) signal at 3680 cm^{-1} (Figure 2b) were missing in the experimental spectra. The calculated O-C-O features were in a definitely worse agreement with IRRAS (see Table 1). Hence, we ruled out bridging bidentate formate from further consideration. To explore alternative proton locations, we built a new model for monodentate formate, with the proton in a subsurface positon (see SI, Figure S1g). Yet upon optimization this adduct converted into the already excluded bridging bidentate, with a subsurface νOH at 3471 cm^{-1} (see SI, Figure S1h,i).

Table 1. Position of IR signals (cm^{-1}) for the adducts in Figures 1-2, and harmonic frequencies for the minima in Figures 3.

	ν(C-H)	ν(O-H)	ν(O-C-O)
Experimental[a]	Not reported	Not detected	1647; 1315
First-Principles MD			
Monodentate	2900-3000	1800-2500	1680; 1290
Bridging $HCOO^-(Ti_s)$ and $H^+(O_s)$	2900-3000	3680	1520; 1360
Harmonic Frequencies			
undissociated **(II)**	3014	2370	1653; 1442
shared-H **(III)**	2983	1676	1530; 1359
dissociated **(I)**	2959	2295	1570;1346

[a] Experimental data[9] included for comparison refer to monodentate species on non-defective (101) anatase.

As the molecule-surface proton-shuttling may be relevant for HCOOH reactivity, we calculated the free energy path[16] for this process at 50 K and 300 K (Figure 3a). In both cases, we found two free energy minima, corresponding to dissociated (**I**) and undissociated (**II**) forms. The barrier is very small (0.84 and 1.17 kcal×mol^{-1} at 50 and 300 K, respectively). In term of kT (Figure 3b) the barrier (8.5 kT at 50 K) amounts to only 2.0 kT at 300 K, hence proton shuttling can occur at room conditions. Also, temperature copes to reduce the thermodynamic stability gap between the two forms (6.4 kT at 50 K, 0.9 kT at 300 K).

Starting from the 50 K profile, we calculated energy minima (at 0 K) at different levels of theory. With PBE,[11] energy differences are modest, with a preference for form **II** by 0.67 kcal×mol^{-1} and a (0 K) barrier of 0.75 kcal×mol^{-1}. With dispersion corrections,[17] form **II** is more stable by 0.48 kcal×mol^{-1} and the barrier is 0.68 kcal×mol^{-1}. Such trend is not quantitatively confirmed by the PBE0[18] data, predicting form **I** more stable by 0.88 kcal×mol^{-1} and a barrier of 0.95 kcal×mol^{-1}. However, the PBE0 results confirm that the energy difference for these structures is limited – indeed, the 0 K energy differences are all within 1 kcal×mol^{-1}.

For the two PBE minima, we calculated the harmonic frequencies (Table 1): in line with the 300 K spectrum, there are no OH signals at wavenumbers > 3000 cm^{-1}, and the νCH modes are at much higher energy. Such low ν(OH) values are due to very strong molecule-surface H-bonding, as indicated by the O_s-O_f separation in the minimum structures **I** and **II** - 2.463 Å and 2.479 Å, respectively.

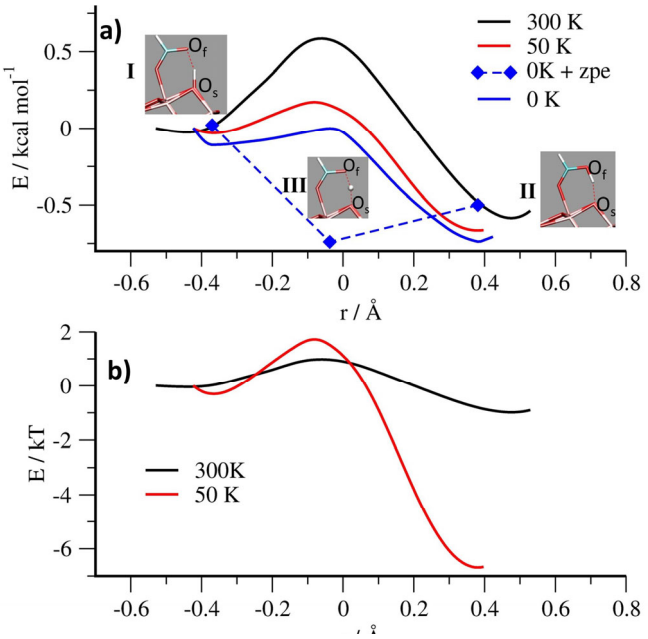

Figure 3. a) Free energy profiles for proton shuttling at 300 K and 50 K. The reaction coordinate r=r(H-O_s)-r(H-O_f) is defined as the difference between the distances of the proton from carboxylate oxygen O_f and surface oxygen O_s (estimated error bar: 0.1 kcal×mol^{-1}). Blue diamonds: zpe-corrected relative energies of the 0 K optimized geometry of the dissociated (**I**), undissociated (**II**) and proton-sharing (**III**) forms. **b)** Free energy profiles in kT-units.

So far, we discussed the thermal behavior of HCOOH on anatase TiO_2 (101) in a classical mechanics frame. Actually, proton transfer events can be influenced by quantum effects,[19–23] in particular by zero point energies (zpe).[22] Although tunnelling may be relevant for intramolecular proton transfers,[24] an overwhelming dominance of zpe effects was demonstrated for intermolecular and/or surface-mediated proton transfers.[20,25] Thus, we optimized the structure of the activated complex **III** at PBE level. The harmonic frequency of the shared proton resulted 1676 cm^{-1} (O_s-O_f distance: 2.395 Å), even lower than those found for the double-well species **I** and **II**. By adding zpe to the energy of the three optimized structures, the barrier disappears (Figure 3a): hence, the quantum approach predicts a shared proton in a single well at 0 K. Yet the energy differences remain below 1 kcal×mol^{-1} even with the zpe contribution. To ascertain whether the proton motion is governed by a single-well or a double-well potential, one should rest on electronic-structure methods with at least 0.1 kcal×mol^{-1} accuracy, which are hardly feasible for systems of this size.[26]

Our study provides useful chemical insight on the surface behavior of carboxylic functionalities. Firstly, both the IR signal due to classic proton shuttling (Figure 2d), and the harmonic frequency for the quantum mechanical minimum (1676 cm^{-1}) fall in the region of strong H-bonds – *i.e.*, below the νCH and very close to the highest O-C-O mode of adsorbed HCOOH. Such information may help experimentalists in identifying shared or shuttling protons from the presence of low-wavenumber, very broad, νOH signals in vibrational spectra of adsorbed carboxylic acids. This model might also explain the reported STM acid proton "invisibility",[10] as the carboxylate group could conceal the proton from the tip. Alternative hypotheses for the lack of proton detection, e.g. desorption of H_2 from the surface, appear less likely due to the low density of Ti interstitial defects on stoichiometric anatase (101).[9,8c]

Secondly, earlier studies suggest that while quantum fluctuations dominate at low temperature, the thermally activated classical behavior should prevail at room temperature.[22,27] To explore this hypothesis, we simulate at 300 K the adsorption of DCOOD, less sensitive than HCOOH to quantum effects.[22,27] This simulation reveals that even the acid deuteron shuttles between TiO_2 and formate (Figure S5). Hence, a classic double-well model may be eligible to describe room temperature HCOOH adsorption on defect-free anatase TiO_2 (101), and might be likely transferrable to stoichiometric anatase nanoparticles mainly terminated by {101} facets, with defects mostly localized at edges and corners.[4,8]

Thirdly, both quantum and classical pictures predict that HCOOH on TiO_2 anatase is essentially neutral (see SI, Table S2). Hence, its reactivity may be different from that of a negatively charged formate and a surface OH group. The floating proton is encaged between a carboxyl oxygen and a surface oxygen, and it is strongly coupled, both electronically and vibrationally, to the TiO_2 lattice (see Figures S6-S8). So, a SSHB with covalent character is formed, which damps the Brønsted acid functionality of formic acid. This protecting-group role of the surface could explain *e.g.* why carboxylic acids pre-adsorbed on TiO_2 nanoparticles undergo amidation instead of salt formation upon addition of amines.[3]

In conclusion, we propose a dynamic model of the adsorption of small carboxylic acids on anatase-TiO_2, which is consistent with experiments, and involves either rapid proton shuttling between a carboxylic and a surface oxygen, or proton sharing due to quantum delocalization. Whereas the quantum mechanical picture should dominate at low temperatures, classic molecule-to-surface proton shuttling should prevail at room conditions. In both cases, via SSHB, the acid proton is coupled to both the molecule and TiO_2. SSHBs are considered crucial in enhancing catalytic rates of enzymatic reactions.[28] Hence, two ideas quintessential of organic synthesis (protecting-group) and enzymatic catalysis (SSHB), meld in a new surface chemistry concept, that may help interpreting reactivity and catalytic processes of acid protons and carboxyl groups at material interfaces.

Acknowledgements

FAR2017 Uninsubria is acknowledged for funding. We gratefully thank three anonymous reviewers for insightful comments.

Keywords: density functional calculations • molecular dynamics • surface chemistry • vibrational spectroscopy• zero point energy

[1] a) Y. Ma, X. Wang, Y. Jia, X. Chen, H. Han, C. Li, *Chem. Rev.* **2014**, *114*, 9987; b) A. Fujishima, X. Zhang, D. A. Tryk, *Surf. Sci. Rep.* **2008**, *63*, 515.

[2] F. Schiffmann, J. VandeVondele, J. Hutter, R. Wirz, A. Urakawa, A. Baiker, *J. Phys. Chem. C* **2010**, *114*, 8398.

[3] C. Deiana, Y. Sakhno, M. Fabbiani, M. Pazzi, M. Vincenti, G. Martra, *ChemCatChem* **2013**, *5*, 2832.

[4] a)M. Fabbiani, M. Pazzi, M. Vincenti, G. Tabacchi, E. Fois, G. Martra, *J. Nanosci. Nanotechnol.* **2018**, *18*, 5854; b) G. Martra, C. Deiana, Y. Sakhno, I. Barberis, M. Fabbiani, M. Pazzi, M. Vincenti,

Angew. Chem. Int. Ed. **2014**, *53*, 4671; *Angew. Chem*. **2014**, 126, 4759; c) J.-F. Lambert, *Orig. Life Evol. Biosph.* **2008**, *38*, 211.
[5] J. Balajka, M. A. Hines, W. J. I. DeBenedetti, M. Komora, J. Pavelec, M. Schmid, U. Diebold, *Science* **2018**, *361*, 786.
[6] a)A. Mattsson, S. Hu, K. Hermansson, L. Österlund, *J. Chem. Phys.* **2014**, *140*, 034705; b) A. Mattsson, L. Österlund, *J. Phys. Chem. C* **2010**, *114*, 14121; c) M. J. Tillotson, P. M. Brett, R. A. Bennett, R. Grau-Crespo, *Surf. Sci.* **2015**, *632*, 142.
[7] a)X. Gong, A. Selloni, A. Vittadini, *J. Phys. Chem. B* **2006**, *110*, 2804;b) X. Q. Gong, A. Selloni, *J. Catal.* **2007**, *249*, 134; c) A. Tilocca, A. Selloni, *J. Phys. Chem. B* **2004**, *108*, 4743; d) A. Vittadini, A. Selloni, F. P. Rotzinger, M. Grätzel, *J. Phys. Chem. B* **2000**, *104*, 1300;e) F. Nunzi, F. De Angelis, *J. Phys. Chem. C* **2011**, *115*, 2179;f) L. Kou, T. Frauenheim, A. L. Rosa, E. N. Lima, *J. Phys. Chem. C* **2017**, *121*, 17417;g) K. L. Miller, J. L. Falconer, J. W. Medlin, *J. Catal.* **2011**, *278*, 321; h)Y. Li, Y. Gao, *Langmuir* **2018**, *34*, 546.
[8] a) C. Deiana, M. Minella, G. Tabacchi, V. Maurino, E. Fois, G. Martra, *Phys. Chem. Chem. Phys.* **2013**, *15*, 307;b) C. Deiana, G. Tabacchi, V. Maurino, S. Coluccia, G. Martra, E. Fois, *Phys. Chem. Chem. Phys.* **2013**, *15*, 13391; c) C. Deiana, E. Fois, G. Martra, S. Narbey, F. Pellegrino, G. Tabacchi, *ChemPhysChem* **2016**, *17*, 1956.
[9] M. Xu, H. Noei, M. Buchholz, M. Muhler, C. Wöll, Y. Wang, *Catal. Today* **2012**, *182*, 12.
[10] D. C. Grinter, M. Nicotra, G. Thornton, *J. Phys. Chem. C* **2012**, *116*, 11643.
[11] J. P. Perdew, K. Burke, M. Ernzerhof, *Phys. Rev. Lett.* **1996**, *77*, 3865.
[12] a) R. Car, M. Parrinello, *Phys. Rev. Lett.* **1985**, *55*, 2471; b) CPMD code, IBM Corp. 1990–2019, MPI für Festkörperforschung Stuttgart 1997–2001, **2019**.
[13] a) S. Hu, P. A. Bopp, L. Österlund, P. Broqvist, K. Hermansson, *J. Phys. Chem. C* **2014**, *118*, 14876; b) C. Spreafico, F. Schiffmann, J. VandeVondele, *J. Phys. Chem. C* **2014**, *118*, 6251; c) E. Fois, G. Tabacchi, D. Barreca, A. Gasparotto, E. Tondello, *Angew. Chem. Int. Ed.* **2010**, *49*, 1944; *Angew. Chem.* **2010**, *122*, 1988; d) L. Martínez-Suarez, N. Siemer, J. Frenzel, D. Marx, *ACS Catal.* **2015**, *5*, 4201;e) G. Tabacchi, E. Fois, G. Calzaferri, *Angew. Chem. Int. Ed*. **2015**, *54*, 11112; *Angew. Chem*. **2015**, *127*, 11264; f) G. Tabacchi, G. Calzaferri, E. Fois, *Chem. Commun.* **2016**, *52*, 11195; g R. Arletti, E. Fois, L. Gigli, G. Vezzalini, S. Quartieri, G. Tabacchi, *Angew. Chem. Int. Ed*. **2017**, 56, 2105; *Angew. Chem.* **2017**, *129*, 2137;h) Y. Fang, D. Lesnicki, K. J. Wall, M.-P. Gaigeot, M. Sulpizi, V. Vaida, V. H. Grassian, *J. Phys. Chem. A* **2019**, *123*, 983.
[14] K. Nakamoto, M. Margoshes, R. E. Rundle, *J. Am. Chem. Soc.* **1955**, *77*, 6480.
[15] a) F. Fontaine-Vive, M. R. Johnson, G. J. Kearley, J. A. K. Howard, S. F. Parker, *J. Am. Chem. Soc.* **2006**, *128*, 2963; b) M. Gadermann, D. Vollmar, R. Signorell, *Phys. Chem. Chem. Phys.* **2007**, *9*, 4535; c) M. Wiebcke, G. Engelhardt, J. Felsche, P. B. Kempa, P. Sieger, J. Schefer,P. Fischer, *J. Phys. Chem.* **1992**, *96*, 392; d) E. Fois, A. Gamba, *J. Phys. Chem. B* **1997**, *101*, 4487; e)J. Lu, I. Hung, A. Brinkmann, Z. Gan, X. Kong, G. Wu, *Angew. Chem. Int. Ed.* **2017**, *56*, 6166; *Angew. Chem*. **2017**, *129*, 6262.
[16] E. A. Carter, G. Ciccotti, J. T. Hynes, R. Kapral, *Chem. Phys. Lett.* **1989**, *156*, 472.
[17] S. Grimme, *J. Comput. Chem.* **2006**, *27*, 1787.
[18] C. Adamo, V. Barone, *J. Chem. Phys.* **1999**, *110*, 6158.
[19] a)W. Caminati, W. Li, L. Evangelisti, Q. Gou, R. Meyer, *Angew. Chem. Int. Ed.* **2019**, *58*, 859; *Angew. Chem*. **2019**, *131*, 869; b)N. Kungwan, C. Ngaojampa, Y. Ogata, T. Kawatsu, Y. Oba, Y. Kawashima, M. Tachikawa, *J. Phys. Chem. A* **2017**, *121*, 7324.
[20] S. D. Ivanov, I. M. Grant, D. Marx, *J. Chem. Phys.* **2015**, *143*, 124304.
[21] D. A. Thomas, M. Marianski, E. Mucha, G. Meijer, M. A. Johnson, G. von Helden, *Angew. Chem. Int. Ed.* **2018**, *57*, 10615; *Angew. Chem.* **2018**, *130*, 10775.
[22] C. Drechsel-Grau, D. Marx, *Phys. Chem. Chem. Phys.* **2017**, *19*, 2623.
[23] a)M. E. Tuckerman, D. Marx, M. Parrinello, *Nature* **2002**, *417*, 925;b) M. Hellström, M. Ceriotti, J. Behler, *J. Phys. Chem. B* **2018**, *122*, 10158; c) I. Frank, *ChemistrySelect* **2019**, *4*, 868; d) P. Kraus, I. Frank, *Chem. Eur. J.* **2018**, *24*, 7188.
[24] a) D. Jose, A. Datta, *Angew. Chem. Int. Ed.* **2012**, *51*, 9389; *Angew. Chem.* **2012**,*124*, 9523; b) A. Fernández-Ramos, *Angew. Chem. Int. Ed.* **2013**, *52*, 8204; *Angew. Chem.* **2013**, *125*, 8362; c) A. Datta, *Angew. Chem. Int. Ed.* **2013**, *52*, 8206; *Angew. Chem.* **2013**, *125*, 8364; d) P. Durlak, Z. Latajka, *J. Comp. Chem.* **2019**, 40, 671.
[25] Y. Litman, D. Donadio, M. Ceriotti, M. Rossi, *J. Chem. Phys.* **2018**, *148*, 102320.
[26] C. Qu, J. M. Bowman, *Phys. Chem. Chem. Phys.* **2019**, *21*, 3397.
[27] C. Drechsel-Grau, D. Marx, *Angew. Chem. Int. Ed.* **2014**, *53*, 10937; *Angew. Chem*. **2014**, *126*, 11117; b) C. Drechsel-Grau, D. Marx, *Phys. Rev. Lett.* **2014**, *112*, 148302; c) C. Schran, O. Marsalek, T. E. Markland, *Chem. Phys. Lett.* **2017**, *678*, 289.
[28] a)W. W. Cleland, M. M. Kreevoy, *Science* **1994**, *264*, 1887; b) A. Langkilde, S. M. Kristensen, L. Lo Leggio, A. Mølgaard, J. H. Jensen, A. R. Houk, J.-C. Navarro Poulsen, S. Kauppinen, S. Larsen, *Acta Crystallogr. Sect. D Biol. Crystallogr.* **2008**, *64*, 851; c) P. Kumar, E. H. Serpersu, M. J. Cuneo, *Sci. Adv.* **2018**, *4*, eaas8667.